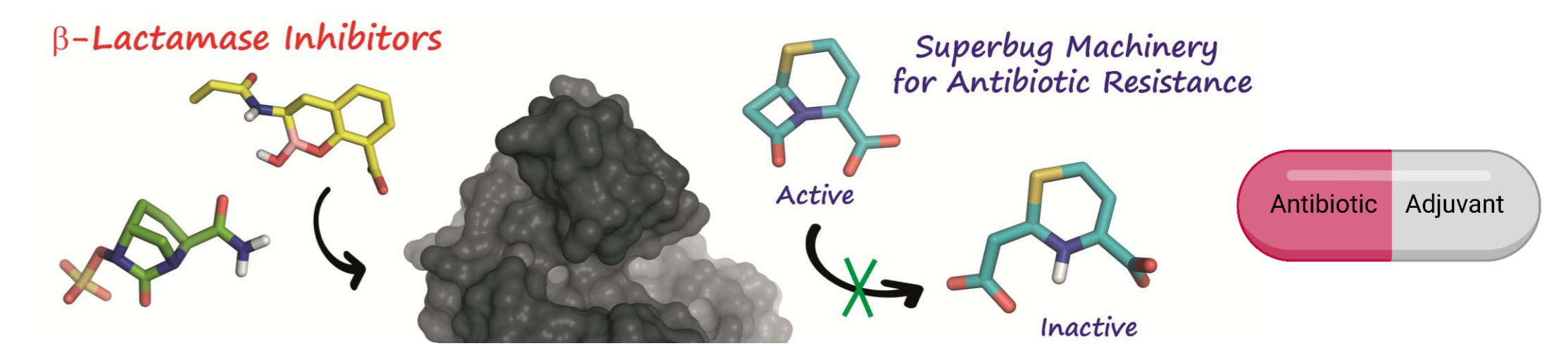


## PRECISION MEDICINE AGAINST BACTERIAL RESISTANCE TO ANTIBIOTICS

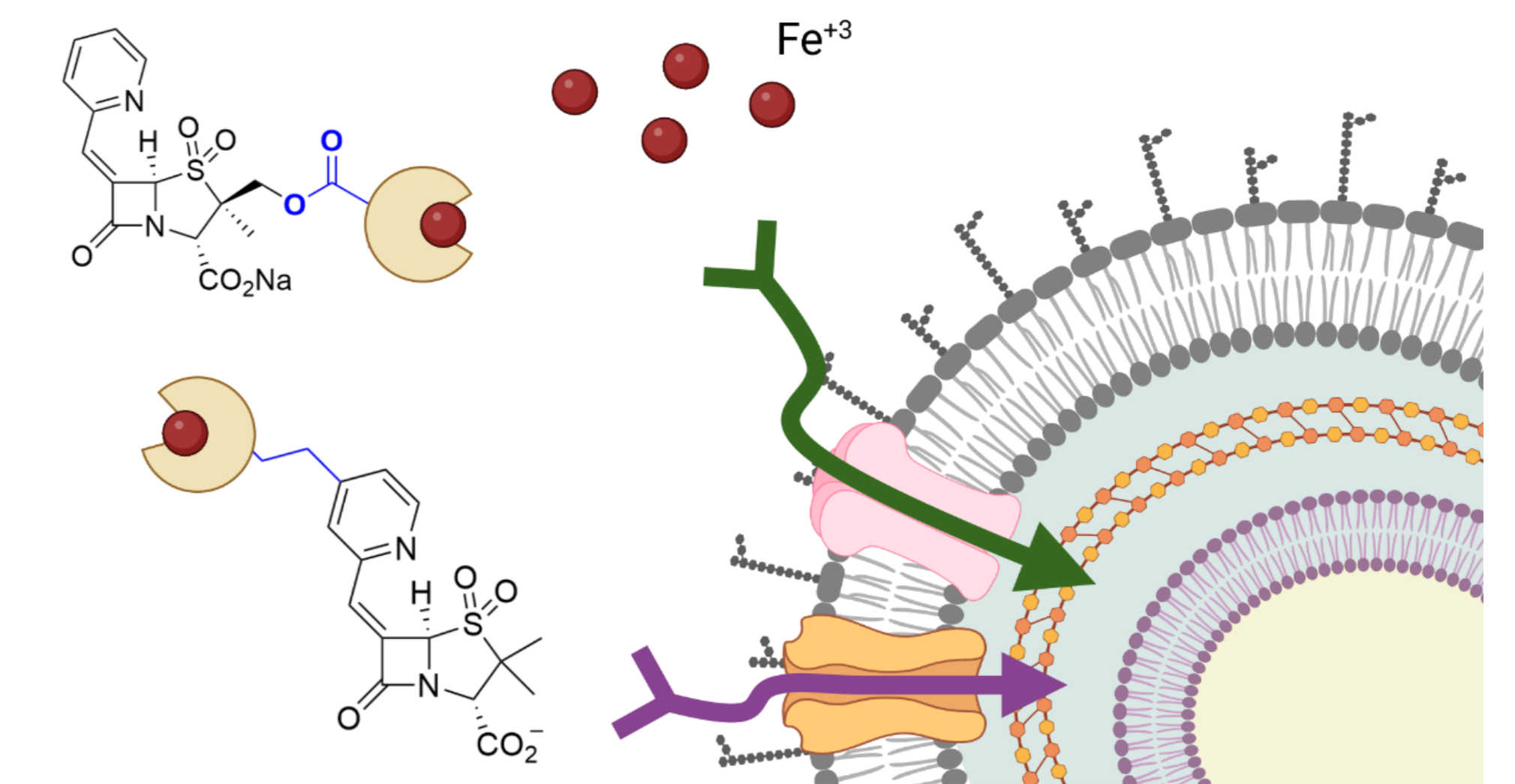
Membrane permeability is a natural defense barrier that contributes to increased bacterial drug resistance, particularly for Gram-negative critical priority pathogens *P. aeruginosa*, *A. baumannii*, and *Enterobacteriales*. As such, accurate delivery of the antibacterial agent to the target has become a growing research area in the infectious diseases field as a means of improving drug efficacy. Although the efficient transport of siderophore-antibiotic conjugates into the cytosol still remains challenging, great success has been achieved in the delivery of  $\beta$ -lactam antibiotics into the periplasmic space via bacterial iron uptake pathways [1]. Cefiderocol, the first siderophore-cephalosporin conjugate approved by the US Food and Drug Administration, is a good example [2]. Huge efforts are currently being devoted to developing  $\beta$ -lactamase inhibitors that are able to reduce the impact of the main bacterial resistance mechanism, thus, hydrolysis of  $\beta$ -lactam antibiotics catalyzed by  $\beta$ -lactamase enzymes. These conjugation strategies were applied to the precise delivery of  $\beta$ -lactamase inhibitors, penicillin-based sulfones, to restore  $\beta$ -lactam antibiotic efficacy in multidrug-resistant bacteria [3,4]. These compounds have a unique mechanism of action. Thus, when binding to the enzyme active site a nucleophilic attack by the catalytic serine residue to generate an indolizine adduct, which is stable against hydrolysis, is obtained.

### GOALS

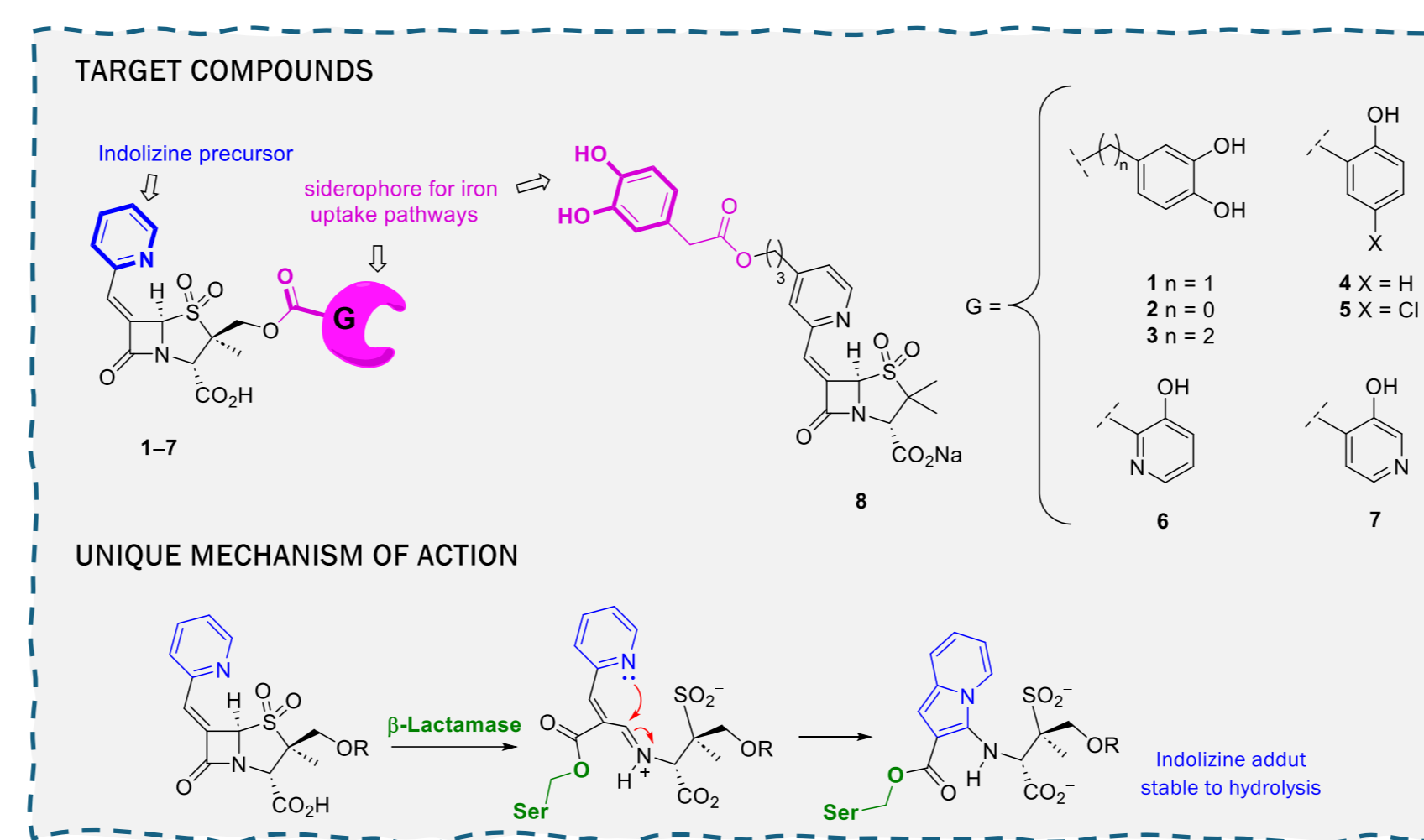
- ✓ To explore the impact on the bacterial activity of diverse penicillin-based sulfones siderophore conjugates, compounds 1–8.
- ✓ *In vitro* evaluation with multidrug-resistant pathogens producing challenging  $\beta$ -lactamases and with isolated enzymes
- ✓ To know the molecular basis of the inhibitory properties of the most relevant compound by molecular dynamics simulation studies.



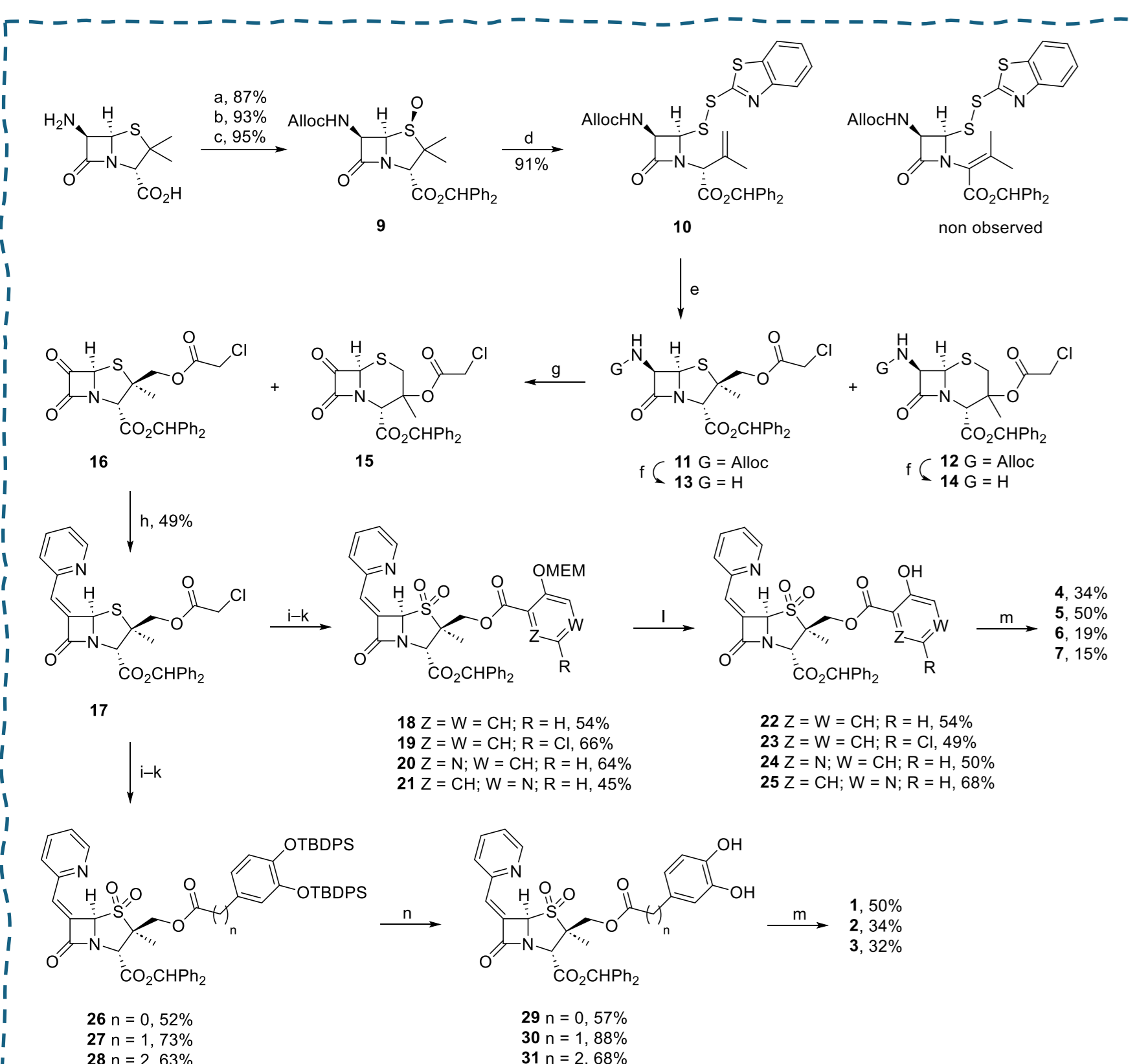
### Minimize the Impact of Bacterial Resistance to Antibiotics



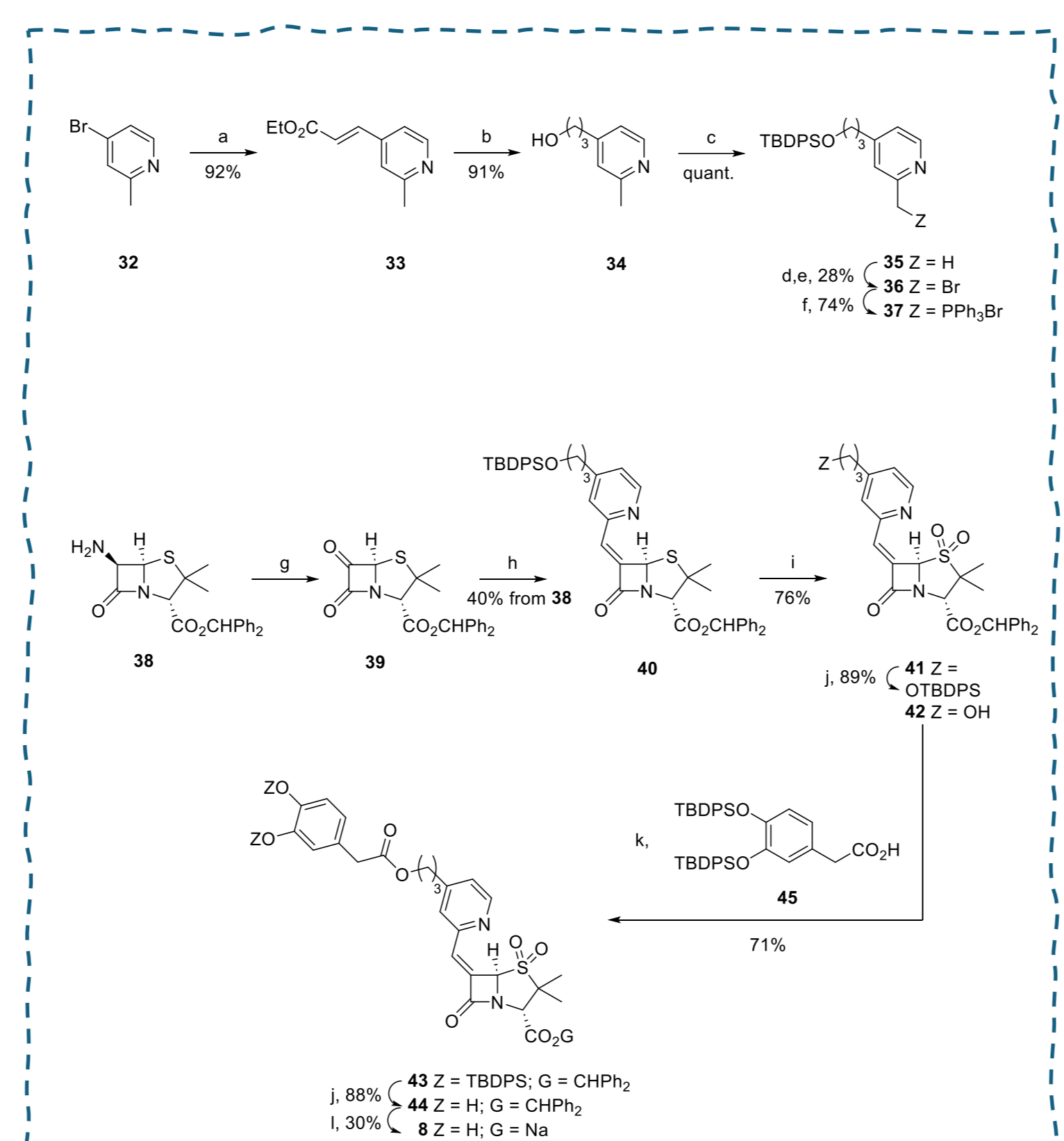
### Precise Delivery for Restoring Carbapenem Efficacy



## SYNTHESIS OF TARGET COMPOUNDS 1 - 8



**Scheme 1.** (a)  $\text{Ph}_3\text{CN}_2$ ,  $\text{CH}_2\text{Cl}_2/\text{MeOH}$ , RT. (b)  $\text{CICO}_2\text{Allyl}$ ,  $\text{Py}$ ,  $\text{CH}_2\text{Cl}_2$ ,  $-10^\circ\text{C}$ . (c)  $\text{MeCO}_2\text{H}$ ,  $\text{CH}_2\text{Cl}_2$ ,  $-5^\circ\text{C}$ . (d) 2-mercaptobenzothiazole,  $\text{MgSO}_4$ , dioxane,  $\Delta$ . (e)  $\text{ClCH}_2\text{CO}_2\text{H}$ ,  $\text{AgOAc}$ ,  $\text{AcOEt}$ , RT. (f)  $\text{Bu}_3\text{SnH}$ ,  $\text{Pd}(\text{PPh}_3)_4$  (cat.),  $\text{AcOH}$ , DCM, RT, 86% from 10. (g)  $\text{Ti}_2\text{O}$ ,  $\text{Et}_3\text{N}$ , DCM,  $-78^\circ\text{C}$  to  $0^\circ\text{C}$ .  $\text{Et}_3\text{N}$ ,  $-78^\circ\text{C}$ . 3.  $\text{HCl}$  (0.5 M). (h) 2-pyridylmethyltriphenylphosphonium bromide, DCM,  $-78^\circ\text{C}$  or RT. (i) MCPBA, DCM, RT. (j) Thiourea,  $\text{Py}$ , DMF,  $0^\circ\text{C}$  to RT. (k)  $\text{ArCO}_2\text{H}$ , EDC, DMAP, DCM,  $-15^\circ\text{C}$  to RT. (l) PPTS,  $\text{tBuOH}$ , RT. (m) 1. m-cresol,  $50^\circ\text{C}$ . 2.  $\text{NaHCO}_3$  (aq.). (n) TBAF,  $\text{AcOH}$ , THF,  $0^\circ\text{C}$ .



**Scheme 2.** (a) ethyl acrylate,  $\text{Pd}(\text{OAc})_2$ ,  $\text{P}(\text{t}-\text{Bu})_3$ ,  $\text{Et}_3\text{N}$ , DMF,  $100^\circ\text{C}$ . (b)  $\text{NaBH}_4$ ,  $\text{MeOH}$ ,  $0^\circ\text{C}$  to  $80^\circ\text{C}$ . (c) TBDPSCl, imidazole, DMF, RT. (d) 1. MCPBA,  $\text{CH}_2\text{Cl}_2$ , RT. 2.  $\text{Ac}_2\text{O}$ ,  $90^\circ\text{C}$ . 3.  $\text{KOH}$ ,  $\text{MeOH}$ ,  $0^\circ\text{C}$  to RT. (e)  $\text{CBr}_4$ ,  $\text{Ph}_3\text{P}$ ,  $\text{CH}_2\text{Cl}_2$ ,  $0^\circ\text{C}$ . (f)  $\text{Ph}_3\text{P}$ ,  $\text{PhMe}$ ,  $\Delta$ . (g)  $\text{Ti}_2\text{O}$ ,  $\text{Et}_3\text{N}$ ,  $\text{CH}_2\text{Cl}_2$ ,  $-78^\circ\text{C}$  to  $0^\circ\text{C}$ .  $\text{Et}_3\text{N}$ ,  $-78^\circ\text{C}$ . 3.  $\text{HCl}$  (0.5 M),  $-78^\circ\text{C}$  to RT. (h) 1. 45,  $\text{tBuOK}$ , THF, RT. 2. 45, DCM,  $-78^\circ\text{C}$ . (i) MCPBA, DCM, RT. (j) TBAF,  $\text{AcOH}$ , THF,  $0^\circ\text{C}$ . (k) 51, EDC, DMAP, DCM,  $-15^\circ\text{C}$  to RT. (l) 1. m-cresol,  $50^\circ\text{C}$ . 2.  $\text{NaHCO}_3$  (aq.).

## SIMULATION STUDIES WITH OXA-48 AND PDC-1

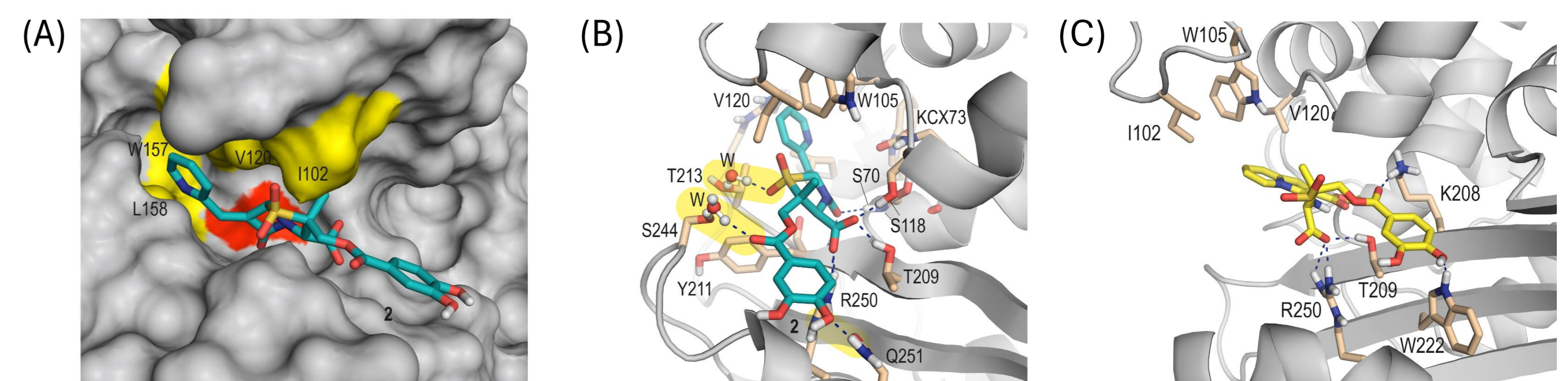


**Figure 1.** Binding mode of inhibitor 2 (blue) to the OXA-48 active site for the acylation reaction (A,B) and inactivated by 2 (C) obtained by MD simulation studies. The large hydrophobic region near the active site (yellow), which is the OXA-48 enzyme feature, and the position of the catalytic serine residue (red) are highlighted.

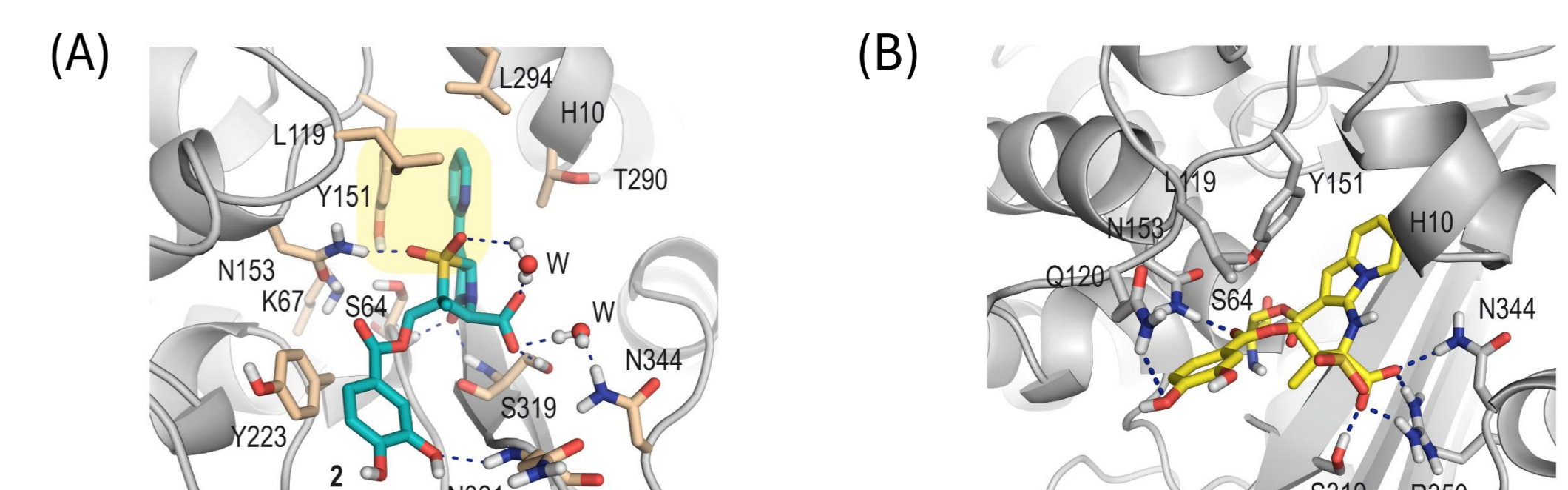


**Figure 2.** Binding mode of inhibitor 2 (blue) to the PDC-1 active site for the acylation reaction (A) and inactivated by 2 (B) obtained by MD simulation studies.

## SUSCEPTIBILITY AND KINETIC STUDIES

**Table 1.** MIC Values ( $\mu\text{g mL}^{-1}$ ) for Ampicillin, Cefazidime, and Imipenem with Several Bacterial Strains Carrying Representative  $\beta$ -Lactamases of Classes A (CTX-M-14), C (CTX-M-2, CMY-2, DHA-1, FOX-4, and PDC-1), and D (OXA-23, OXA-24/40, and OXA-48) in the Presence and Absence of  $\beta$ -Lactamase Inhibitors 1–8 and Avibactam<sup>a</sup>

bacterial strain and type of $\beta$ -lactamase produced	Class A		Class C				Class D		OXA-48
	CTX-M-14	CTX-M-2	CMY-2	DHA-1	FOX-4	PDC-1	OXA-23	OXA-24/40	
ESBL	ESBL	ESBL	ESBL	ESBL	ESBL	ESBL	carbapenemase	carbapenemase	carbapenemase
antibiotic used without an inhibitor	AMP	CAZ	CAZ	CAZ	CAZ	CAZ	IP	IP	IP
avibactam	NA	NA	NA	NA	NA	1	4	16	NA
1	16	$\leq 1$	$\leq 0.06$	$\leq 0.06$	$\leq 0.06$	1	0.5	0.5	4
2	4	$\leq 1$	$\leq 0.06$	$\leq 0.06$	$\leq 0.06$	1	0.5	0.5	2
3	32	2	$\leq 0.06$	$\leq 0.06$	0.12	1	0.5	1	16
4	256	64	0.12	0.25	2	2	2	16	16
5	512	64	0.12	0.12	16	2	2	16	16
6	1024	512	4	16	32	8	8	64	64
7	1024	256	1	4	0.12	4	4	32	16
8	1024	256	4	8	8	8	4	32	32
without $\beta$ -lactamase	2	2	$\leq 0.06$	$\leq 0.06$	$\leq 0.06$	1	0.5	0.5	0.5

<sup>a</sup>Inhibitor concentration =  $16 \mu\text{g mL}^{-1}$ ; AMP = ampicillin; CAZ = cefazidime; IP = imipenem; NA = not applicable (avibactam shows antimicrobial activity against these strains); yellow shadow = susceptibility increased relative to 1; blue shadow = susceptibility maintained relative to 1.

**Table 2.** Inhibition Kinetics of OXA-23, OXA-48, and PDC-1 by Compounds 1, 2, and 9 and Avibactam<sup>a</sup>

enzyme	inhibitor	$\text{IC}_{50}$ ( $\mu\text{M}$ )	$K_{\text{app}}$ ( $\mu\text{M}$ )	$K_i$ ( $\mu\text{M}$ )	$k_{\text{app}}$ ( $\text{s}^{-1}$ )	$k_{\text{inact}}/K_i$ ( $\text{M}^{-1} \text{s}^{-1}$ )
OXA-23	1	$0.012 \pm 0.008$	$0.088 \pm 0.006$	$0.30 \pm 0.08$	$0.041 \pm 0.005$	$1.4 \times 10^5 \pm 0.3 \times 10^5$
	2	$0.051 \pm 0.012$	$0.817 \pm 0.274$	$0.716 \pm 0.061$	$0.040 \pm 0.002$	$5.7 \times 10^4 \pm 0.5 \times 10^4$
	AVI	$8.93 \pm 0.99$	$105.56 \pm 3.08$	$203.93 \pm 22.6$	$0.057 \pm 0.009$	$2.9 \times 10^3 \pm 0.6 \times 10^3$
OXA-48	1	$0.003 \pm 0.0003$	$0.17 \pm 0.01$	ND	ND	ND
	2	$0.013 \pm 0.002$	$0.045 \pm 0.007$	$0.131 \pm 0.011$	$0.045 \pm 0.004$	$3.4 \times 10^5 \pm 0.3 \times 10^5$
	AVI	$0.852 \pm 0.051$	$9.830 \pm 2.612$	$38.918 \pm 14.601$	$0.086 \pm 0.010$	$2.4 \times 10^3 \pm 0.8 \times 10^3$
PDC-1	1	$0.0061 \pm 0.0019$	$0.053 \pm 0.019$	$0.0748 \pm 0.0189$	$0.046 \pm 0.006$	$6.3 \times 10^5 \pm 1.4 \times 10^5$
	2	$0.0013 \pm 0.0002$	$0.005 \pm 0.001$	$0.0113 \pm 0.0019$	$0.032 \pm 0.005$	$2.9 \times 10^6 \pm 0.8 \times 10^6$
	AVI	$0.0510 \pm 0.0031$	$0.990 \pm 0.075$	ND	ND	ND

<sup>a</sup>ND = not determined because the maximum  $k_{\text{app}}$  required to calculate the parameter was not reached; AVI = avibactam.

## CONCLUSIONS

- Compound 2, which contains a catechol group linked to the pro-S methyl of the sulfone scaffold via an aromatic ester, is the best inhibitor of the series.
- Compound 2 is a  $\beta$ -lactamase inhibitor with an expanded spectrum of activity.
- The susceptibility of ampicillin in combination with 2 against *E. coli* and *K. pneumoniae* producing ESBL CTX-M-14 and OXA-48, respectively was increased.
- *In silico* studies have shown that the linkage of the catechol group via an aromatic ester appears to promote extra key interactions with the residues of the active site, thus reducing the flexibility obtained with compound 1.
- The aromatic ester linkage improves internalization into the periplasmic space.

## REFERENCES

- Rodríguez, D.; González-Bello, C. *Bioorg. Med. Chem. Lett.* **2023**, *87*, 129282.
- González-Bello, C.; Rodríguez, D.; Pernas, M.; Rodríguez, A.; Colchón, E. *J. Med. Chem.* **2020**, *63*, 1859.
- Rodríguez, D.; Maneiro, M.; Vázquez-Ucha, J.C.; Beceiro, A.; González-Bello, C. *J. Med. Chem.* **2020**, *63*, 3737.
- Rodríguez, D.; Lence, E.; Vázquez-Ucha, J.C.; Beceiro, A.; González-Bello, C. *ACS Omega* **2024**, *9*, 26484.

## ACKNOWLEDGEMENTS

Financial support from the AEI (PID2019-105512RB-I00, PID2022-136963OB-I00), the Xunta de Galicia [ED431C 2025/05 and Centro singular de investigación de Galicia accreditation 2024–2027 (ED431G 2023/03)] and the European Regional Development Fund is acknowledged. We are grateful to the Centro de Supercomputación de Galicia (CESGA) for use of the Finis Terrae computer.

